

New physics contributions to $\bar{B}_s \rightarrow \pi^0(\rho^0)\eta^{(\prime)}$ decays

Gaber Faisel^{1,2,*}

¹*Department of Physics, Faculty of Arts and Sciences,
Süleyman Demirel University, Isparta, Turkey 32260.*

²*Department of Physics, National Taiwan University, Taipei, Taiwan 10617.*

Abstract

The decay modes $\bar{B}_s \rightarrow \pi^0(\rho^0)\eta^{(\prime)}$ are dominated by electroweak penguins that are small in the standard model. In this work we investigate the contributions to these penguins from a model with an additional $U(1)'$ gauge symmetry and show their effects on the branching ratios of $\bar{B}_s \rightarrow \pi^0(\rho^0)\eta^{(\prime)}$. In a scenario of the model, where Z' couplings to the left-handed quarks vanish, we show that the maximum enhancement occurs in the branching ratio of $\bar{B}_s^0 \rightarrow \pi^0\eta'$ where it can reach 6 times the SM prediction. On the other hand, in a scenario of the model where Z' couplings to both left-handed and right-handed quarks do not vanish, we find that Z' contributions can enhance the branching ratio of $B_s^0 \rightarrow \rho^0\eta$ up to one order of magnitude comparing to the SM prediction for several sets of the parameter space where both ΔM_{B_s} and $S_{\psi\phi}$ constraints are satisfied. This kind of enhancement occurs for a rather fine-tuned point where ΔM_{B_s} constraint on $|S_{SM}(B_s) + S_{Z'}(B_s)|$ is fulfilled by overcompensating the SM via $S_{Z'}(B_s) \simeq -2S_{SM}(B_s)$.

* gaberfaisel@sdu.edu.tr

I. INTRODUCTION

The purely isospin-violating decays $\bar{B}_s \rightarrow \phi \pi (\rho^0)$, $\bar{B}_s \rightarrow \pi \eta(\eta')$ and $\bar{B}_s \rightarrow \rho^0 \eta(\eta')$ are dominated by the electroweak penguins[1–4]. These penguins are small in the standard model and can serve as a probe of new physics beyond the standard model. The decay modes $\bar{B}_s \rightarrow \phi \pi (\rho^0)$ have been studied within SM in different frameworks such as QCD factorization as in Refs.[5, 6], in PQCD as in Ref.[7] and using Soft Collinear Effective Theory (SCET) as in Refs.[8, 9]. The study has been extended to include NP models namely, a modified Z^0 penguin, a model with an additional $U(1)'$ gauge symmetry and the MSSM using QCDF [6]. In addition, the investigation of NP in these decay modes has been recently extended to include supersymmetric models with non-universal A-term [9] and two Higgs doublet models (2HDMs)[10] using SCET. The results of these studies showed that the additional Z' boson of the $U(1)'$ gauge symmetry with couplings to leptons switched off can lead to an enhancement in their Branching Ratios (BR) up to an order of magnitude making these decays are interesting for LHCb and future B factories searches [6].

Recently tension between the SM and data related to $b \rightarrow s \ell^+ \ell^-$ channels has become apparent. In particular LHCb has reported deviations from the Standard Model predictions in the processes $B \rightarrow K^* \mu^+ \mu^-$ and $B_s \rightarrow \phi \mu^+ \mu^-$ that are mediated by $b \rightarrow s \mu^+ \mu^-$ transition. Moreover the deviations include the process $B \rightarrow K \mu^+ \mu^-$ through the ratio R_K defined as

$$R_K = \frac{Br(B \rightarrow K \mu^+ \mu^-)}{Br(B \rightarrow K e^+ e^-)} \quad (1)$$

These anomalies can be naturally accommodated in Z' models as have been found in Refs.[11–16]. These findings serve as a general phenomenological motivation for Z' models and for the search of analogous tensions in hadronic B decays. In this work we investigate the phenomenological implications of a leptophobic Z' model on the decay modes $\bar{B}_s \rightarrow \pi \eta(\eta')$ and $\bar{B}_s \rightarrow \rho^0 \eta(\eta')$. In this model Z' couplings to quarks are not related to their couplings to leptons and thus can avoid the tight constraints from semileptonic decays [6].

The decay modes $\bar{B}_s \rightarrow \pi \eta(\eta')$ and $\bar{B}_s \rightarrow \rho^0 \eta(\eta')$ have been studied within SM using different frameworks such as Naive Factorization (NF)[2], generalized factorization [3], POCD [7, 17] and QCDF [4, 18]. On the other hand, using SCET, an investigation of $\bar{B}_s \rightarrow \pi \eta(\eta')$ has been carried out in Ref.[19] while the decay modes $\bar{B}_s \rightarrow \rho^0 \eta(\eta')$ has been studied in Ref.[8]. NP effects namely 2HDMs has been investigated in these decay modes in Ref. [2]

Decay mode	T_1	T_2	T_{1g}	T_{2g}
$\bar{B}_s \rightarrow \eta_s \pi^0$	0	$\frac{1}{\sqrt{2}}(c_2^s - c_3^s)$	0	$\frac{1}{\sqrt{2}}(c_2^s - c_3^s)$
$\bar{B}_s \rightarrow \eta_s \rho^0$	0	$\frac{1}{\sqrt{2}}(c_2^s + c_3^s)$	0	$\frac{1}{\sqrt{2}}(c_2^s + c_3^s)$
$\bar{B}_s \rightarrow \eta_q \pi^0$	0	0	0	$(c_2^s - c_3^s)$
$\bar{B}_s \rightarrow \eta_q \rho^0$	0	0	0	$(c_2^s + c_3^s)$

TABLE I. Hard kernels of $\bar{B}_s^0 \rightarrow \eta_{s,q} \pi^0(\rho^0)$ decays. The hard kernels T_{iJ} , T_{iJg} , for $i = 1, 2$, can be obtained through the replacement $c_i^s \rightarrow b_i^s$

using NF and using generalized factorization in Ref. [20]. In our study we will adopt SCET as a framework for the calculation of the amplitudes[21–24].

SCET provides a systematic and rigorous way to deal with the processes in which energetic quarks and gluons have different momenta modes such as hard, soft and collinear modes. The power counting in SCET reduces the complexity of the calculations. In addition, the factorization formula given by SCET is perturbative to all powers in α_s expansion.

This paper is organized as follows. In Sec. II, we review the decay amplitude for $B \rightarrow M_1 M_2$ within SCET framework. Accordingly, we present the SM predictions of the branching ratios of the decay modes under the study in Sec. III. Then we proceed to analyze NP contributions namely the non universal Z' model in section IV. Finally, we give our conclusion in Sec. V.

II. $\bar{B}_s \rightarrow \pi^0(\rho^0) \eta^{(\prime)}$ DECAYS IN SCET

The decay amplitude of B meson into two light final states mesons M_1, M_2 at LO in $\alpha_s(m_b)$ expansion in SCET can be written as [8]:

$$A(B \rightarrow M_1 M_2) = \frac{G_F}{\sqrt{2}} m_B^2 \left\{ f_{M_1} \left[\zeta_J^{BM_2} \int du \phi_{M_1}(u) T_{1J}(u) + \zeta_{Jg}^{BM_2} \int du \phi_{M_1}(u) T_{1Jg}(u) \right] + f_{M_1} (T_1 \zeta^{BM_2} + T_{1g} \zeta_g^{BM_2}) + A_{cc}^{M_1 M_2} + (1 \leftrightarrow 2) \right\}, \quad (2)$$

here $M_1 M_2$ can be PP or PV where P stands for pseudoscalar meson and V stands for vector meson and $\phi_M(u)$ is the light-cone distribution amplitude (LCDA) of the meson M . $A_{cc}^{M_1 M_2}$ represents the non-perturbative long distance charm contribution to the amplitude. The hadronic parameters ζ^{BM} , ζ_g^{BM} , ζ_J^{BM} and ζ_{Jg}^{BM} , in the framework of SCET, are treated as

non-perturbative parameters that can be fitted using the experimental data of the branching fractions and CP asymmetries of the non leptonic B and B_s decays [8, 19, 25, 26]. The hard kernels T_i , T_{ig} , $T_{iJ}(u)$ and $T_{iJg}(u)$ for $i = 1, 2$ are functions of the Wilson coefficients of the weak effective Hamiltonian. The expressions of these kernels for a certain $B \rightarrow M_1 M_2$ decay mode in the case of SM can be obtained using the formulas given in the appendix of Ref.[8].

In many extensions of the SM the weak effective Hamiltonian can have new set of operators \tilde{Q}_i that are obtained by flipping the chirality of the SM four-quark operators from left to right. Following a similar treatment to that in Ref.[8] we find that the effect of these new operators can be incorporated in the expressions of the hard kernels T_i , T_{ig} , $T_{iJ}(u)$ and $T_{iJg}(u)$. In Table (I) we present the explicit expressions of the hard kernels T_i , T_{ig} , $T_{iJ}(u)$ relevant to the decay channels $\bar{B}_s \rightarrow \eta_s \pi^0$, $\bar{B}_s \rightarrow \eta_q \pi^0$, $\bar{B}_s \rightarrow \eta_s \rho^0$ and $\bar{B}_s \rightarrow \eta_q \rho^0$. The Coefficients c_i^s and b_i^s are functions of Wilson coefficients of the weak effective Hamiltonian. After extending the SM weak effective Hamiltonian to include right-handed operators \tilde{Q}_i generated by NP we find that

$$\begin{aligned} c_2^{(s)} &= \lambda_u^{(s)} \left[C_2 - \tilde{C}_2 + \frac{1}{N_c} (C_1 - \tilde{C}_1) \right] - \frac{3}{2} \lambda_t^{(s)} \left[C_9 - \tilde{C}_9 + \frac{1}{N_c} (C_{10} - \tilde{C}_{10}) \right], \\ c_3^{(s)} &= -\frac{3}{2} \lambda_t^{(s)} \left[C_7 - \tilde{C}_7 + \frac{1}{N_c} (C_8 - \tilde{C}_8) \right], \end{aligned} \quad (3)$$

and

$$\begin{aligned} b_2^{(s)} &= \lambda_u^{(s)} \left[C_2 + \tilde{C}_2 + \frac{1}{N_c} \left(1 - \frac{m_b}{\omega_3} \right) (C_1 + \tilde{C}_1) \right] - \frac{3}{2} \lambda_t^{(s)} \left[C_9 + \tilde{C}_9 + \frac{1}{N_c} \left(1 - \frac{m_b}{\omega_3} \right) (C_{10} + \tilde{C}_{10}) \right], \\ b_3^{(s)} &= -\frac{3}{2} \lambda_t^{(s)} \left[C_7 - \tilde{C}_7 + \frac{1}{N_c} \left(1 - \frac{m_b}{\omega_2} \right) (C_8 - \tilde{C}_8) \right], \end{aligned} \quad (4)$$

where $C_i = C_i^{SM} + C_i^{NP}$ and $\tilde{C}_i = \tilde{C}_i^{SM} + \tilde{C}_i^{NP}$. The Wilson coefficients \tilde{C}_i correspond to the four-quark operators in the weak effective Hamiltonian that have right chirality. In the SM such operators are absent and hence $\tilde{C}_i^{SM} = 0$. In Eq.(4) we have $\omega_2 = um_{\bar{B}_s}$ and $\omega_3 = -\bar{u}m_{\bar{B}_s}$ with u is the momentum fraction of the positive quark in the emitted meson and $N_c = 3$. From charge conjugation and isospin we have $\phi_{\pi(\rho)}(u) = \phi_{\pi(\rho)}(1-u)$ [26]. Thus we can write

$$\int_0^1 du \frac{\phi_M(u)}{\bar{u}} = \int_0^1 du \frac{\phi_M(1-u)}{1-u} = \int_0^1 du \frac{\phi_M(u)}{u} = \langle \chi^{-1} \rangle_M \quad (5)$$

for $M = \pi$ and $M = \rho$. This relation together with the relation

$$\int_0^1 du \phi_M(u) = 1 \quad (6)$$

allow us to perform the integrals in eq.(2) and express the results in terms of the hadronic parameter $\langle \chi^{-1} \rangle_M$. For the physical states η and η' they are related to the flavor basis η_s and η_q through [19]:

$$\begin{pmatrix} \eta \\ \eta' \end{pmatrix} = \begin{pmatrix} \cos \phi & -\sin \phi \\ \sin \phi & \cos \phi \end{pmatrix} \begin{pmatrix} \eta_q \\ \eta_s \end{pmatrix}. \quad (7)$$

Where the mixing angle is measured as $\phi = 46^\circ$ [27]. Upon using this relation we can easily calculate the decay amplitudes of $\bar{B}_s \rightarrow \eta M$ and $\bar{B}_s \rightarrow \eta' M$ for $M = \pi$ and $M = \rho$.

III. $\bar{B}_s \rightarrow \pi^0(\rho^0)\eta^{(\prime)}$ DECAYS IN THE STANDARD MODEL

In this section we give our predictions for the branching ratios of $\bar{B}_s \rightarrow \pi^0(\rho^0)\eta^{(\prime)}$ decays in the standard model. In our analysis, we use the different set of values given in Refs.[8] for the hadronic parameters ζ^{BM} , ζ_g^{BM} , ζ_J^{BM} and ζ_{Jg}^{BM} corresponding to the two solutions obtained from the χ^2 fit and assuming a 20% error in their values due to the SU(3) symmetry breaking. It should be noted that the values that enter the SCET predictions are obtained from a fit to data assuming SM Wilson coefficients. They are valid for NP analysis provided the NP contribution to those channels which dominate the fit is small compared to the SM contribution. This is the case for the considered Z' scenarios. We use for the inverse moment of the ρ meson light-cone distribution amplitude $\langle \chi^{-1} \rangle_\rho = 3.45$ [28] and $\langle \chi^{-1} \rangle_\pi = 2.9 \pm 0.4$ [29].

The amplitudes of $\bar{B}_s \rightarrow \pi^0(\rho^0)\eta^{(\prime)}$ decays in the SM can be obtained by setting $\tilde{C}_i^{SM} = C_i^{Z'} = \tilde{C}_i^{Z'} = 0$. For $\bar{B}_s \rightarrow \pi^0\eta^{(\prime)}$ decays we obtain

$$\begin{aligned} \mathcal{A}_1(\bar{B}_s^0 \rightarrow \eta \pi^0) \times 10^6 &\simeq -5.6 C_9^{SM} \lambda_c^s - (2.3 C_1^{SM} + 3.7 C_2^{SM}) \lambda_u^s \\ \mathcal{A}_2(\bar{B}_s^0 \rightarrow \eta \pi^0) \times 10^6 &\simeq -5.1 C_9^{SM} \lambda_c^s - (1.6 C_1^{SM} + 3.4 C_2^{SM}) \lambda_u^s \\ \mathcal{A}_1(\bar{B}_s^0 \rightarrow \eta' \pi^0) \times 10^6 &\simeq 0.4 C_9^{SM} \lambda_c^s + (0.1 C_1^{SM} + 0.3 C_2^{SM}) \lambda_u^s \\ \mathcal{A}_2(\bar{B}_s^0 \rightarrow \eta' \pi^0) \times 10^6 &\simeq 1.8 C_9^{SM} \lambda_c^s + (2.7 C_1^{SM} + 1.2 C_2^{SM}) \lambda_u^s \end{aligned} \quad (8)$$

while for $\bar{B}_s \rightarrow \rho^0\eta^{(\prime)}$ decays we obtain

$$\begin{aligned}
\mathcal{A}_1(\bar{B}_s \rightarrow \eta \rho^0) \times 10^6 &\simeq -6.3 C_9^{SM} \lambda_c^s - (3.4 C_1^{SM} + 4.2 C_2^{SM}) \lambda_u^s \\
\mathcal{A}_2(\bar{B}_s \rightarrow \eta \rho^0) \times 10^6 &\simeq -3.0 C_9^{SM} \lambda_c^s - (1.6 C_1^{SM} + 2.0 C_2^{SM}) \lambda_u^s \\
\mathcal{A}_1(\bar{B}_s \rightarrow \eta' \rho^0) \times 10^6 &\simeq 3.3 C_9^{SM} \lambda_c^s + (0.8 C_1^{SM} + 2.2 C_2^{SM}) \lambda_u^s \\
\mathcal{A}_2(\bar{B}_s \rightarrow \eta' \rho^0) \times 10^6 &\simeq 8.2 C_9^{SM} \lambda_c^s + (6.3 C_1^{SM} + 5.4 C_2^{SM}) \lambda_u^s
\end{aligned} \tag{9}$$

where we have used the unitarity of the CKM matrix to write $\lambda_t^s = -\lambda_u^s - \lambda_c^s$ and also the hierarchy of the SM Wilson coefficients $C_1^{SM} \gg C_i^{SM}$ for $i = 2, 3, 4, 5, 6, 7, 8, 9, 10$ and $C_9^{SM} \gg C_i^{SM}$ for $i = 7, 8, 10$. The amplitudes \mathcal{A}_1 and \mathcal{A}_2 refers to solutions 1 and 2 of the SCET parameters respectively. From the CKM matrix we can write to a good approximation $\lambda_c^s \simeq Re(\lambda_c^s) \simeq 0.04$ and $|\lambda_u^s| \simeq 2 \times 10^{-2} \lambda_c^s$. At leading order we have

$$C_1^{SM} = 1.1, \quad C_2^{SM} = -0.253, \quad C_9^{SM} = -10.3 \times 10^{-3} \tag{10}$$

Clearly the real parts of the amplitudes in Eqs(8,9) are dominant by the terms proportional to $C_9^{SM} \lambda_c^s \simeq -4 \times 10^{-4}$. This can be attributed to several reasons. First, the cancellation that take places in the λ_u^s terms of the amplitudes due to the sign difference between C_1^{SM} and C_2^{SM} . Second, the sign difference between the terms proportional to λ_c^s and λ_u^s after taking into account the minus sign of the Wilson coefficient C_9^{SM} . And finally due to the hierarchy $|\lambda_u^s| \simeq 2 \times 10^{-2} \lambda_c^s$. Another remark, the imaginary parts of the amplitudes in Eqs(8,9) are suppressed as they are proportional to $|\lambda_u^s| \simeq 2 \times 10^{-2} \lambda_c^s \simeq 10^{-4}$. As a consequence the predicted branching ratios for these decay modes are small as shown in Table (II). The last two columns give the predictions corresponding to the two solutions of the SCET parameters obtained from the χ^2 fit. The errors on the SCET predictions are due to SU(3) breaking effects and errors due to SCET parameters respectively.

IV. Z' MODEL CONTRIBUTIONS TO $\bar{B}_s \rightarrow \pi^0(\rho^0) \eta^{(\prime)}$ DECAYS

One of the possible extension of the SM is to enlarge the SM gauge group to include additional $U(1)'$ gauge group. This possibility is well-motivated in several beyond SM theories such as theories with large extra dimensions[30] and grand unified theories[31]. As a consequence of the $U(1)'$ gauge symmetry a new gauge boson, Z' , arises. Basically Z' can

Decay channel	QCDF	PQCD	SCET solution 1	SCET solution 2
$\bar{B}_s \rightarrow \eta \pi^0$	$0.075^{+0.013+0.030+0.008+0.010}_{-0.012-0.025-0.010-0.007}$	$0.05^{+0.02+0.01+0.00}_{-0.02-0.01-0.00}$	$0.037^{+0.010+0.006}_{-0.010-0.006}$	$0.031^{+0.009+0.003}_{-0.009-0.003}$
$\bar{B}_s \rightarrow \eta' \pi^0$	$0.11^{+0.02+0.04+0.01+0.01}_{-0.02-0.04-0.01-0.01}$	$0.11^{+0.05+0.02+0.00}_{-0.03-0.01-0.00}$	$0.0002^{+0.001+0.001}_{-0.001-0.001}$	$0.033^{+0.010+0.010}_{-0.010-0.010}$
$\bar{B}_s \rightarrow \eta \rho^0$	$0.17^{+0.03+0.07+0.02+0.02}_{-0.03-0.06-0.02-0.01}$	$0.06^{+0.03+0.01+0.00}_{-0.02-0.01-0.00}$	$0.055^{+0.018+0.017}_{-0.018-0.017}$	$0.012^{+0.009+0.004}_{-0.009-0.004}$
$\bar{B}_s \rightarrow \eta' \rho^0$	$0.25^{+0.06+0.10+0.02+0.02}_{-0.05-0.08-0.02-0.02}$	$0.13^{+0.06+0.02+0.00}_{-0.04-0.02-0.01}$	$0.013^{+0.009+0.016}_{-0.009-0.016}$	$0.148^{+0.045+0.043}_{-0.045-0.043}$

TABLE II. Branching ratios of $\bar{B}_s^0 \rightarrow \eta^{(\prime)} \pi^0$ and $\bar{B}_s \rightarrow \eta^{(\prime)} \rho^0$ decays in 10^{-6} units. The last two columns give the predictions corresponding to the two solutions of the SCET parameters obtained from the χ^2 fit. On the SCET predictions the errors are due to SU(3) breaking effects and errors due to SCET parameters respectively. For a comparison with previous studies in the literature, we list the results evaluated in QCDF [5], PQCD [7].

have either family universal couplings or family non-universal couplings to the SM fermions. In the case that Z' gauge couplings are family universal they remain diagonal even in the presence of fermion flavor mixing by the GIM mechanism[32]. On the other hand and in some models like string models it is possible to have family-non universal Z' couplings, due to the different constructions of the different families[32–35]. This scenario with family-non universal couplings has theoretical and phenomenological motivations. For instance, possible anomalies in the Z -pole $b\bar{b}$ asymmetries suggest that the data are better fitted with a non-universal Z' [36]. Recent studies about the phenomenology of Z' has been performed in Refs.[13, 37–43]. For a detailed review about the physics of Z' gauge-bosons we refer to Ref.[44].

In our analysis we will follow Refs. [6, 13, 36–43, 45–51] and consider a non-universal Z' couplings in a way independent to a specific Z' model. Neglecting Z - Z' mixing and assuming the absence of exotic fermions that can mix with the SM fermions through the Z' couplings, the quark-antiquark- Z' interaction Lagrangian can be written as [6, 45, 49]

$$\mathcal{L}_{Z'}^{eff} = -\frac{g_{U(1)'}}{2\sqrt{2}} \sum_{ij} \bar{q}_i [\zeta_L^{ij} \gamma^\mu (1 - \gamma_5) + \zeta_R^{ij} \gamma^\mu (1 + \gamma_5)] q_j Z'_\mu. \quad (11)$$

where i and j denote different quark flavours of the same type quarks. In order to simplify our analysis we introduce the parameters

$$i\Delta_{L,R}^{ij} \equiv -\frac{g_{U(1)'}}{\sqrt{2}} \zeta_{L,R}^{ij} \quad (12)$$

In terms of these parameters we find that Z' contributions to the electroweak penguins relevant to our decay processes, at the electroweak scale, are given as

$$\begin{aligned} C_7^{Z'} &= \frac{4}{3} \frac{M_W^2 \Delta_L^{sb}}{g^2 M_{Z'}^2 \lambda_t^{(s)}} (\Delta_R^{uu} - \Delta_R^{dd}) , & \tilde{C}_7^{Z'} &= \frac{4}{3} \frac{M_W^2 \Delta_R^{sb}}{g^2 M_{Z'}^2 \lambda_t^{(s)}} (\Delta_L^{uu} - \Delta_L^{dd}) , \\ C_9^{Z'} &= \frac{4}{3} \frac{M_W^2 \Delta_L^{sb}}{g^2 M_{Z'}^2 \lambda_t^{(s)}} (\Delta_L^{uu} - \Delta_L^{dd}) , & \tilde{C}_9^{Z'} &= \frac{4}{3} \frac{M_W^2 \Delta_R^{sb}}{g^2 M_{Z'}^2 \lambda_t^{(s)}} (\Delta_R^{uu} - \Delta_R^{dd}) . \end{aligned} \quad (13)$$

The $SU(2)_L$ invariance implies that $\zeta_L^{uu} = \zeta_L^{dd}$ [6]. As a consequence $\Delta_L^{uu} = \Delta_L^{dd}$ and thus we are left with only two non-vanishing coefficients

$$\begin{aligned} C_7^{Z'} &= \frac{4}{3} \frac{M_W^2 \Delta_L^{sb}}{g^2 M_{Z'}^2 \lambda_t^{(s)}} (\Delta_R^{uu} - \Delta_R^{dd}) , \\ \tilde{C}_9^{Z'} &= \frac{4}{3} \frac{M_W^2 \Delta_R^{sb}}{g^2 M_{Z'}^2 \lambda_t^{(s)}} (\Delta_R^{uu} - \Delta_R^{dd}) . \end{aligned} \quad (14)$$

Last equation indicates that Z' contributions to the Electroweak Wilson coefficients vanish in the case of $\Delta_R^{uu} = \Delta_R^{dd} = 0$ or $\Delta_R^{uu} = \Delta_R^{dd}$.

We discuss now the constraints imposed on the $\Delta_{L,R}^{ij}$ parameters. To avoid tight constraints from semileptonic decays we consider Z' model with vanishing couplings to leptons. In this model Z' mass is much less constrained [6]. This can be explained as leptophobic Z' bosons can avoid detection via traditional Drell-Yan processes. This choice can be adopted as the couplings of the Z' boson to quarks are not related to their couplings to leptons. This leptophobic Z' boson can appear in models with an E_6 gauge symmetry [52].

The most stringent constraints on the couplings Δ_L^{sb} and Δ_R^{sb} stem from $B_s - \bar{B}_s$ mixing. The effective Hamiltonian governs $B_s - \bar{B}_s$ mixing can be written as [38, 53, 54]

$$\mathcal{H}_{eff}^{\Delta f=2} = C_1^{VLL} Q_1^{VLL} + C_1^{VRR} Q_1^{VRR} + C_1^{LR} Q_1^{LR} + C_2^{LR} Q_2^{LR} \quad (15)$$

where the four-quark operators are given as

$$\begin{aligned} Q_1^{VLL} &= [\bar{b}_\alpha \gamma^\mu P_L s_\alpha] [\bar{b}_\beta \gamma^\mu P_L s_\beta] , \\ Q_1^{VRR} &= [\bar{b}_\alpha \gamma^\mu P_R s_\alpha] [\bar{b}_\beta \gamma^\mu P_R s_\beta] , \\ Q_1^{LR} &= [\bar{b}_\alpha \gamma^\mu P_L s_\alpha] [\bar{b}_\beta \gamma^\mu P_R s_\beta] , \\ Q_2^{LR} &= [\bar{b}_\alpha P_L s_\alpha] [\bar{b}_\beta P_R s_\beta] , \end{aligned} \quad (16)$$

The $\Delta B_s = 2$ mass difference is given as [38]

$$\Delta M_{B_s} = \frac{G_F^2}{6\pi^2} M_W^2 m_{B_s} |\lambda_t^s|^2 F_{B_s}^2 \hat{B}_{B_s} \eta_B |S(B_s)| \quad (17)$$

The expression of $S(B_s)$ can be expressed as [38]

$$S(B_s) = S_0(x_t) + [\Delta S(B_s)]_{VLL} + [\Delta S(B_s)]_{VRR} + [\Delta S(B_s)]_{LR} \equiv |S(B_s)| e^{i\theta_S^{B_s}} \quad (18)$$

where the loop function $S_0(x_t)$ stems from the SM contribution to the $\Delta B_s = 2$ mass difference

$$S_0(x_t) = \frac{4x_t - 11x_t^2 + x_t^3}{4(1-x_t)^2} - \frac{3x_t^2 \log x_t}{2(1-x_t)^3} \quad (19)$$

with $x_t = \frac{m_t^2}{m_W^2}$. The rest of quantities in $S(B_s)$ account for Z' contribution to the $\Delta B_s = 2$ mass difference. The expressions for $[\Delta S(B_s)]_{VLL(VRR)}$ are given as [38]

$$[\Delta S(B_s)]_{VLL(VRR)} = \left[\frac{\Delta_{L(R)}^{bs}}{\lambda_t^s} \right]^2 \frac{4\tilde{r}}{M_{Z'}^2 g_{SM}^2} \quad (20)$$

Here \tilde{r} is a factor that accounts for QCD renormalization group effects. Explicit expressions for \tilde{r} and g_{SM}^2 can be found in Ref.[39]. Turning now to the expression of $[\Delta S(B_s)]_{LR}$ one finds that [38]

$$[\Delta S(B_s)]_{LR} = \frac{\Delta_L^{bs} \Delta_R^{bs}}{M_{Z'}^2 T(B_s)} [C_1^{LR}(\mu_{Z'}) \langle Q_1^{LR}(\mu_{Z'}, B_s) \rangle + C_2^{LR}(\mu_{Z'}) \langle Q_2^{LR}(\mu_{Z'}, B_s) \rangle] \quad (21)$$

where

$$\begin{aligned} T(B_s) &= \frac{G_F^2}{12\pi^2} M_W^2 m_{B_s} |\lambda_t^s|^2 F_{B_s}^2 \hat{B}_{B_s} \eta_B \\ C_1^{LR}(\mu_{Z'}) &= 1 + \frac{\alpha_s}{4\pi} \left(-\log \frac{M_{Z'}^2}{\mu_{Z'}^2} - \frac{1}{6} \right), \\ C_2^{LR}(\mu_{Z'}) &= \frac{\alpha_s}{4\pi} \left(-6 \log \frac{M_{Z'}^2}{\mu_{Z'}^2} - 1 \right). \end{aligned} \quad (22)$$

The central values of the matrix elements $\langle Q_{1,2}^{LR}(\mu_{Z'}, B_s) \rangle$ can be found in Table 1 in Ref.[38]. In order to take the experimental and the hadronic uncertainties into account we follow Ref.[38] and require that the theory to reproduce the data for ΔM_{B_s} within $\pm 5\%$. Thus for $\Delta M_{B_s}^{Exp} = 17.761(22) \text{ ps}^{-1}$ [55] the allowed range reads

$$16.9/\text{ps} \leq \Delta M_{B_s} \leq 18.6/\text{ps} \quad (23)$$

The previous relation can be used to set constraints on the parameters $\Delta_{L,R}^{bs}$ once the values of $M_{Z'}$ are given. The most stringent constraints on $M_{Z'}$ are provided by CMS experiment [56]. For the sequential Z' model the lower bound for $M_{Z'}$ is 2.59 TeV while in other models values as low as 1 TeV are still possible.

In addition to the constraint from ΔM_{B_s} we need to take into account the constraint from $S_{\psi\phi}$ which can be defined as [38]

$$S_{\psi\phi} = \sin(2|\beta_s| - 2\phi_{B_s}) \quad (24)$$

where the phases β_s and ϕ_{B_s} are defined by

$$V_{ts} = -|V_{ts}|e^{-i\beta_s}, \quad 2\phi_{B_s} = -\theta_S^{B_s} \quad (25)$$

with $\beta_s \simeq -1^\circ$ and $\theta_S^{B_s}$ is the phase of $S(B_s)$ given in Eq.(18). The LHCb measurement of $S_{\psi\phi}$ reads [57]

$$S_{\psi\phi} = 0.002 \pm 0.087 \quad (26)$$

To use $S_{\psi\phi}$ as a constraint on the parameter space, we follow Ref.[38] and require $S_{\psi\phi}$ to vary in the range

$$-0.18 \leq S_{\psi\phi} \leq 0.18 \quad (27)$$

In our analysis we will consider two scenarios. In the first scenario, the Right-Handed Scenario (RHS), we assume $\Delta_R^{ij} \neq 0$ and $\Delta_L^{ij} = 0$. Note that the scenario with $\Delta_L^{ij} \neq 0$ and $\Delta_R^{ij} = 0$ is not interesting for our decay modes as this scenario leads to the vanishing of the Wilson coefficients. In the second scenario, the Left-Right Scenario (LRS), we assume $\Delta_R^{ij} \neq 0$ and $\Delta_L^{ij} \neq 0$. In Ref.[38] a scenario with a left-right symmetry in the Z' -couplings to quarks i.e. $\Delta_L^{ij} = \Delta_R^{ij}$ has been adopted. This scenario is not relevant to our decay modes as it leads to vanishing Z' contributions to the amplitudes. This can be explained as the $SU(2)_L$ invariance implies that $\Delta_L^{uu} = \Delta_L^{dd}$ and hence $\Delta_R^{uu} - \Delta_R^{dd} = \Delta_L^{uu} - \Delta_L^{dd} = 0$ leading to vanishing $C_7^{Z'}$ and $\tilde{C}_9^{Z'}$. Thus in our LRS scenario we take $\Delta_L^{ij} \neq \Delta_R^{ij}$.

We start our analysis by investigating the parameter space in the two scenarios. In the RHS the parameter space consists of the points $(M_{Z'}, Re(\Delta_R^{bs}), Im(\Delta_R^{bs}))$. For a given value of $M_{Z'}$ we can use the constraints from ΔM_{B_s} and $S_{\psi\phi}$ to show the allowed regions in the $Re(\Delta_R^{bs}) - Im(\Delta_R^{bs})$ plane. In Fig.(1) left, we plot the allowed regions in the $Re(\Delta_R^{bs}) -$

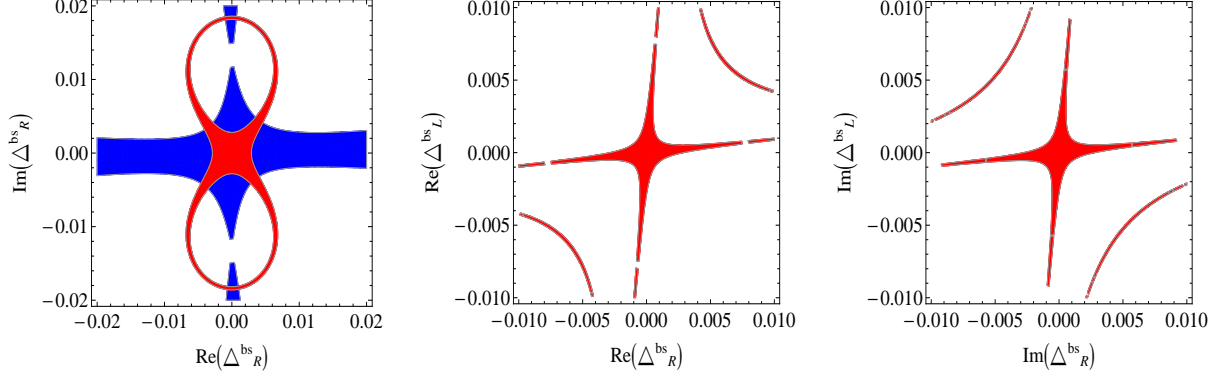


FIG. 1. Left: allowed regions in the $Re(\Delta_R^{bs}) - Im(\Delta_R^{bs})$ plane in RHS where red (blue) color corresponds to the bounds on ΔM_{B_s} ($S_{\psi\phi}$). Middle: allowed regions in $Re(\Delta_R^{bs}) - Re(\Delta_L^{bs})$ plane in LRS from the bounds on ΔM_{B_s} corresponding to the case $Im(\Delta_L^{bs}) = Im(\Delta_R^{bs}) = 0$. Right: allowed regions in the $Im(\Delta_R^{bs}) - Im(\Delta_L^{bs})$ plane in LRS from the bounds on ΔM_{B_s} corresponding to the case $Re(\Delta_L^{bs}) = Re(\Delta_R^{bs}) = 0$. In all plots we take $M_{Z'} = 1$ TeV

$Im(\Delta_R^{bs})$ plane for a value of $M_{Z'} = 1$ TeV. The red (blue) color corresponds to the allowed regions from the bounds on ΔM_{B_s} ($S_{\psi\phi}$). Clearly from the figure combining both constraints reduces the allowed regions in the $Re(\Delta_R^{bs}) - Im(\Delta_R^{bs})$ plane.

We turn now to the LRS. The parameter space in this case consists of the points the $(M_{Z'}, Re(\Delta_L^{bs}), Im(\Delta_L^{bs})), (Re(\Delta_R^{bs}), Im(\Delta_R^{bs}))$. For a given value of $M_{Z'}$ we can use the constraints from ΔM_{B_s} and $S_{\psi\phi}$ to find the allowed regions in the $(Re(\Delta_L^{bs}), Im(\Delta_L^{bs}), Re(\Delta_R^{bs}), Im(\Delta_R^{bs}))$ space. In Fig.(1) middle we show the allowed regions in the $Re(\Delta_R^{bs}) - Re(\Delta_L^{bs})$ from the bounds on ΔM_{B_s} at $M_{Z'} = 1$ TeV corresponding to case $Im(\Delta_L^{bs}) = Im(\Delta_R^{bs}) = 0$. There is no bound from $S_{\psi\phi}$ in this case. In the same figure right we show the allowed regions in the $Im(\Delta_R^{bs}) - Im(\Delta_L^{bs})$ plane in LRS from the bounds on ΔM_{B_s} corresponding to case $Re(\Delta_L^{bs}) = Re(\Delta_R^{bs}) = 0$. Regarding the bounds from $S_{\psi\phi}$, for this case, we find that they are so loose. This can be explained as Z' contribution to ΔM_{B_s} is dominated by the new LR operators which become real in this case and hence the phase $\theta_S^{B_s} \simeq 0$. In addition to the previous two cases in the LRS there is a general case where non of the real or imaginary parts of Δ_L^{bs} and Δ_R^{bs} is equal to zero. In Table III we list some sample sets that satisfy both ΔM_{B_s} and $S_{\psi\phi}$ constraints at $M_{Z'} = 1$ TeV corresponding to this general case. In obtaining these sets we run each of the real and imaginary parts of Δ_L^{bs} and Δ_R^{bs} over the interval $[-0.01, 0.01]$ and require both ΔM_{B_s} and $S_{\psi\phi}$ constraints to be satisfied. Having discussed

Set	$Re(\Delta_L^{bs})$	$Im(\Delta_L^{bs})$	$Re(\Delta_R^{bs})$	$Im(\Delta_L^{bs})$
I	-0.01	-0.01	-0.001	-0.001
II	-0.01	0.005	-0.001	0.0005
III	0.002	0.005	0.0005	0.0005
IV	0.0035	0.002	0.0065	-0.0055
V	0.005	0.005	0.0005	0.0005

TABLE III. Sample sets of the parameter space at $M_{Z'} = 1$ TeV that satisfy both ΔM_{B_s} and $S_{\psi\phi}$ constraints.

the parameter space we proceed to estimate the predictions for the Z' Wilson coefficients and accordingly the branching ratios.

We see from Eq.(14) that the Wilson coefficients $C_7^{Z'}$ and $\tilde{C}_9^{Z'}$ depend on the difference $\Delta_R^{uu} - \Delta_R^{dd}$. Clearly $C_7^{Z'}$ and $\tilde{C}_9^{Z'}$ will vanish if the couplings ζ_R^{qq} , and hence Δ_R^{qq} , are universal. On the other hand the maximum values of the Wilson coefficients $C_7^{Z'}$ and $\tilde{C}_9^{Z'}$ correspond to the maximum value of the coupling difference $\Delta_R^{uu} - \Delta_R^{dd}$. In our analysis we assume that the difference $\Delta_R^{uu} - \Delta_R^{dd}$ is real and $\Delta_R^{uu} - \Delta_R^{dd} = 1$ to get an estimation of the upper values of the branching ratios of $\bar{B}_s \rightarrow \pi^0(\rho^0)\eta^{(\prime)}$.

In the *RHS* scenario $\Delta_L^{sb} = 0$ and $\Delta_R^{sb} \neq 0$. As a result $C_7^{Z'} = 0$ and $\tilde{C}_9^{Z'} \neq 0$. This means that Z' contributes to the amplitude of the given decay process only through the non-vanishing $\tilde{C}_9^{Z'}$.

The amplitudes of $\bar{B}_s \rightarrow \pi^0 \eta^{(\prime)}$ including Z' contributions then become

$$\begin{aligned}
\mathcal{A}_1(\bar{B}_s^0 \rightarrow \eta \pi^0) \times 10^6 &\simeq -(5.6 - 1.8 Re(\frac{\tilde{C}_9^{Z'}}{C_9^{SM}}) - 1.8 Im(\frac{\tilde{C}_9^{Z'}}{C_9^{SM}})I)C_9^{SM} \lambda_c^s - (2.3 C_1^{SM} + 3.7 C_2^{SM})\lambda_u^s \\
\mathcal{A}_2(\bar{B}_s^0 \rightarrow \eta \pi^0) \times 10^6 &\simeq -(5.1 - 3.3 Re(\frac{\tilde{C}_9^{Z'}}{C_9^{SM}}) - 3.3 Im(\frac{\tilde{C}_9^{Z'}}{C_9^{SM}})I)C_9^{SM} \lambda_c^s - (1.6 C_1^{SM} + 3.4 C_2^{SM})\lambda_u^s \\
\mathcal{A}_1(\bar{B}_s^0 \rightarrow \eta' \pi^0) \times 10^6 &\simeq (0.4 - 0.3 Re(\frac{\tilde{C}_9^{Z'}}{C_9^{SM}}) - 0.3 Im(\frac{\tilde{C}_9^{Z'}}{C_9^{SM}})I)C_9^{SM} \lambda_c^s + (0.1 C_1^{SM} + 0.3 C_2^{SM})\lambda_u^s \\
\mathcal{A}_2(\bar{B}_s^0 \rightarrow \eta' \pi^0) \times 10^6 &\simeq (1.8 + 6.6 Re(\frac{\tilde{C}_9^{Z'}}{C_9^{SM}}) + 6.6 Im(\frac{\tilde{C}_9^{Z'}}{C_9^{SM}})I)C_9^{SM} \lambda_c^s + (2.7 C_1^{SM} + 1.2 C_2^{SM})\lambda_u^s
\end{aligned} \tag{28}$$

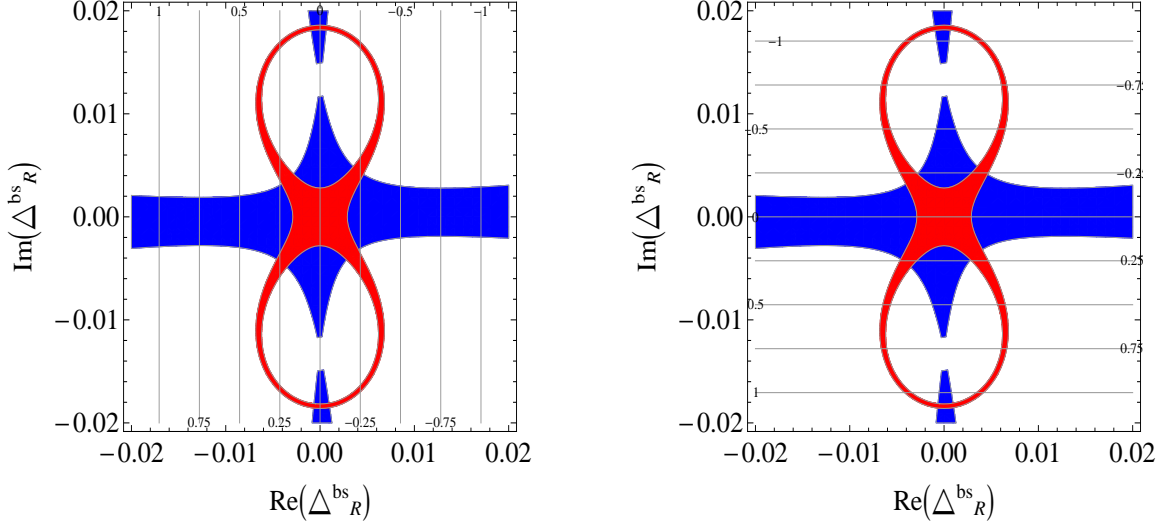


FIG. 2. Left (right): contours of the real (imaginary) part of $\tilde{C}_9^{Z'}$ normalized by the SM Wilson coefficient C_9^{SM} in the RHS. The shaded red (blue) region is allowed from the bounds on ΔM_{B_s} ($S_{\psi\phi}$) for $M_{Z'} = 1$ TeV.

while for $\bar{B}_s \rightarrow \rho^0 \eta^{(\prime)}$ decays we obtain

$$\begin{aligned}
\mathcal{A}_1(\bar{B}_s \rightarrow \eta \rho^0) \times 10^6 &\simeq -(6.3 - 0.3 \text{Re}(\frac{\tilde{C}_9^{Z'}}{C_9^{SM}}) - 0.3 \text{Im}(\frac{\tilde{C}_9^{Z'}}{C_9^{SM}})I) C_9^{SM} \lambda_c^s - (3.4 C_1^{SM} + 4.2 C_2^{SM}) \lambda_u^s \\
\mathcal{A}_2(\bar{B}_s \rightarrow \eta \rho^0) \times 10^6 &\simeq -(3.0 - 0.1 \text{Re}(\frac{\tilde{C}_9^{Z'}}{C_9^{SM}}) - 0.1 \text{Im}(\frac{\tilde{C}_9^{Z'}}{C_9^{SM}})I) C_9^{SM} \lambda_c^s - (1.6 C_1^{SM} + 2.0 C_2^{SM}) \lambda_u^s \\
\mathcal{A}_1(\bar{B}_s \rightarrow \eta' \rho^0) \times 10^6 &\simeq (3.3 - 3.1 \text{Re}(\frac{\tilde{C}_9^{Z'}}{C_9^{SM}}) - 3.1 \text{Im}(\frac{\tilde{C}_9^{Z'}}{C_9^{SM}})I) C_9^{SM} \lambda_c^s + (0.8 C_1^{SM} + 2.2 C_2^{SM}) \lambda_u^s \\
\mathcal{A}_2(\bar{B}_s \rightarrow \eta' \rho^0) \times 10^6 &\simeq (8.2 + 5.2 \text{Re}(\frac{\tilde{C}_9^{Z'}}{C_9^{SM}}) + 5.2 \text{Im}(\frac{\tilde{C}_9^{Z'}}{C_9^{SM}})I) C_9^{SM} \lambda_c^s + (6.3 C_1^{SM} + 5.4 C_2^{SM}) \lambda_u^s
\end{aligned} \tag{29}$$

We discuss now the predictions of $\tilde{C}_9^{Z'}$. In Fig.(2) we show the contours of the real and imaginary parts of $\tilde{C}_9^{Z'}$ normalized by the SM Wilson coefficient C_9^{SM} . The shaded red (blue) region is allowed from the bounds on ΔM_{B_s} ($S_{\psi\phi}$) for a value of $M_{Z'} = 1$ TeV. As can be seen from the figure, the real part of $\tilde{C}_9^{Z'}$ can reach a maximum value of about 25% of the SM Wilson coefficient C_9^{SM} . On the other hand the imaginary part of $\tilde{C}_9^{Z'}$ can reach a maximum value equal to C_9^{SM} at the point $(\text{Re}(\Delta_R^{bs}) = 0, \text{Im}(\Delta_R^{bs}) = \pm 0.018)$ in the same figure. At this point we find that $S_{\psi\phi} \simeq 0.035$ satisfying the $S_{\psi\phi}$ bound in Eq.(27). Moreover, at the same point, we find that $[\Delta S(B_s)]_{VRR} = -4.4 \simeq -2 S_0(x_t)$ i.e. $S_{Z'}(B_s) \simeq -2 S_{SM}(B_s)$. Thus

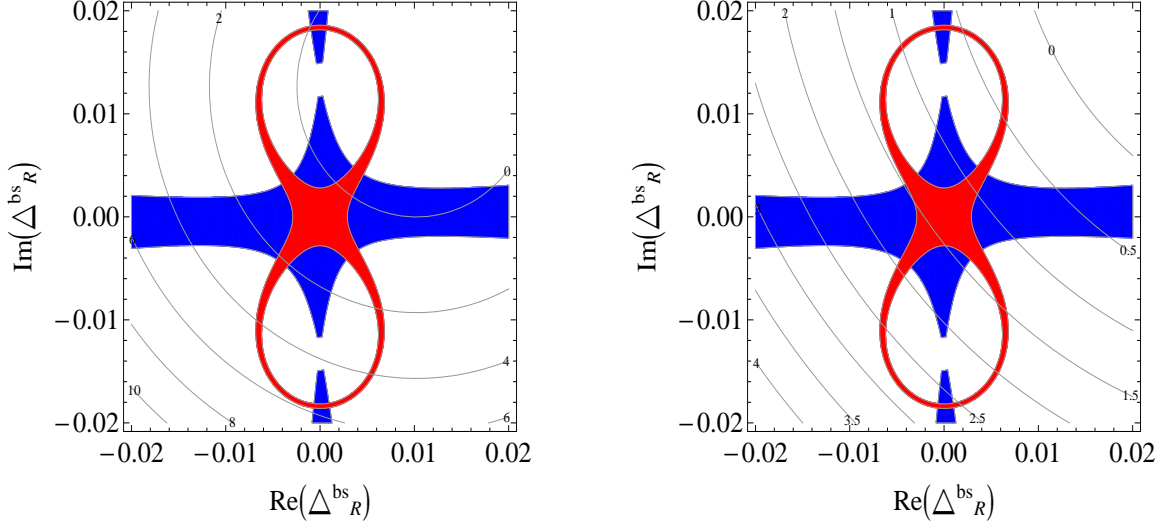


FIG. 3. Left (right): contours of $\mathcal{R}_2^{\pi^0 \eta'}$ ($\mathcal{R}_2^{\rho^0 \eta'}$) in the RHS. The shaded red (blue) region is allowed from the bounds on ΔM_{B_s} ($S_{\psi\phi}$) for $M_{Z'} = 1$ TeV.

$|S_{SM}(B_s) + S_{Z'}(B_s)| \simeq |-S_{SM}(B_s)|$ and thus the point ($Re(\Delta_R^{bs}) = 0, Im(\Delta_R^{bs}) = \pm 0.018$) satisfies ΔM_{B_s} constraint.

As can be seen from Eqs.(28, 29) the decay amplitudes $\mathcal{A}_2(\bar{B}_s^0 \rightarrow \eta' \pi^0)$ and $\mathcal{A}_2(\bar{B}_s \rightarrow \eta' \rho^0)$ have the largest coefficients of the real and imaginary parts of $\tilde{C}_9^{Z'}$ compared to the other amplitudes. Thus we expect that these amplitudes receive the largest enhancements due to $\tilde{C}_9^{Z'}$ and consequently their branching ratios. We define the ratio $\mathcal{R}_i^{M_1 M_2} = (BR_i^{SM+Z'}(\bar{B}_s \rightarrow M_1 M_2) - BR_i^{SM}(\bar{B}_s \rightarrow M_1 M_2)) / BR_i^{SM}(\bar{B}_s \rightarrow M_1 M_2)$ where $i = 1, 2$ refers to solutions 1, 2 for the SCET parameter space and BR refers to the branching ratio. The numerical value of $\mathcal{R}_i^{M_1 M_2}$ gives an estimation of the size of the enhancement or the suppression in the branching ratios due to the contributions of Z' to the amplitude of the given decay process. In Fig.(3) left (right) we show the contours of $\mathcal{R}_2^{\pi^0 \eta'}$ ($\mathcal{R}_2^{\rho^0 \eta'}$) over the allowed regions in the $Re(\Delta_R^{bs}) - Im(\Delta_R^{bs})$ plane, satisfying both $S_{\psi\phi}$ and ΔM_{B_s} constraints, for a value of $M_{Z'} = 1$ TeV. We see from Fig.(3) left that $\mathcal{R}_2^{\pi^0 \eta'}$ can reach a maximum value of about 6 at the point ($Re(\Delta_R^{bs}) = 0, Im(\Delta_R^{bs}) = -0.018$). This means that at this point Z' contributions can enhance the total branching ratio of $\bar{B}_s^0 \rightarrow \pi^0 \eta'$ to six times the SM prediction. Recall that at this point $S_{\psi\phi} \simeq 0.035$ satisfying the $S_{\psi\phi}$ bound in Eq.(27) and $S_{Z'}(B_s) \simeq -2S_{SM}(B_s)$ resulting in $|S_{SM}(B_s) + S_{Z'}(B_s)| \simeq |-S_{SM}(B_s)|$ and thus ΔM_{B_s} constraint is also satisfied. On the other hand from Fig.(3) right we see that $\mathcal{R}_2^{\rho^0 \eta'}$ can reach

a maximum value of only about 2.5 also at the point $(Re(\Delta_R^{bs}) = 0, Im(\Delta_R^{bs}) = -0.018)$. Thus the enhancement in the total branching ratio of the decay mode $B_s^0 \rightarrow \rho^0 \eta'$ is not much compared to the enhancement in decay mode $\bar{B}_s^0 \rightarrow \pi^0 \eta'$.

We consider now LRS scenario in which $\Delta_L^{sb} \neq 0$ and $\Delta_R^{sb} \neq 0$. As a consequence $C_7^{Z'} \neq 0$ and $\tilde{C}_9^{Z'} \neq 0$ and hence the amplitudes of $\bar{B}_s \rightarrow \pi^0 \eta^{(\prime)}$ can be written as

$$\begin{aligned} \mathcal{A}_1(\bar{B}_s^0 \rightarrow \eta \pi^0) \times 10^6 &\simeq (5.6 C_7^{Z'} - 5.6 C_9^{SM} + 1.8 \tilde{C}_9^{Z'}) \lambda_c^s - (2.3 C_1^{SM} + 3.7 C_2^{SM}) \lambda_u^s \\ \mathcal{A}_2(\bar{B}_s^0 \rightarrow \eta \pi^0) \times 10^6 &\simeq (5.1 C_7^{Z'} - 5.1 C_9^{SM} + 3.3 \tilde{C}_9^{Z'}) \lambda_c^s - (1.6 C_1^{SM} + 3.4 C_2^{SM}) \lambda_u^s \\ \mathcal{A}_1(\bar{B}_s^0 \rightarrow \eta' \pi^0) \times 10^6 &\simeq (-0.4 C_7^{Z'} + 0.4 C_9^{SM} - 0.3 \tilde{C}_9^{Z'}) \lambda_c^s + (0.1 C_1^{SM} + 0.3 C_2^{SM}) \lambda_u^s \\ \mathcal{A}_2(\bar{B}_s^0 \rightarrow \eta' \pi^0) \times 10^6 &\simeq (-1.8 C_7^{Z'} + 1.8 C_9^{SM} + 6.6 \tilde{C}_9^{Z'}) \lambda_c^s + (2.7 C_1^{SM} + 1.2 C_2^{SM}) \lambda_u^s \end{aligned} \quad (30)$$

while for $\bar{B}_s \rightarrow \rho^0 \eta^{(\prime)}$ decays we obtain

$$\begin{aligned} \mathcal{A}_1(\bar{B}_s \rightarrow \eta \rho^0) \times 10^6 &\simeq (-11.4 C_7^{Z'} - 6.3 C_9^{SM} + 0.3 \tilde{C}_9^{Z'}) \lambda_c^s - (3.4 C_1^{SM} + 4.2 C_2^{SM}) \lambda_u^s \\ \mathcal{A}_2(\bar{B}_s \rightarrow \eta \rho^0) \times 10^6 &\simeq (-13.3 C_7^{Z'} - 3.0 C_9^{SM} + 0.1 \tilde{C}_9^{Z'}) \lambda_c^s - (1.6 C_1^{SM} + 2.0 C_2^{SM}) \lambda_u^s \\ \mathcal{A}_1(\bar{B}_s \rightarrow \eta' \rho^0) \times 10^6 &\simeq (-1.9 C_7^{Z'} + 3.3 C_9^{SM} - 3.1 \tilde{C}_9^{Z'}) \lambda_c^s + (0.8 C_1^{SM} + 2.2 C_2^{SM}) \lambda_u^s \\ \mathcal{A}_2(\bar{B}_s \rightarrow \eta' \rho^0) \times 10^6 &\simeq (-2.6 C_7^{Z'} + 8.2 C_9^{SM} + 5.2 \tilde{C}_9^{Z'}) \lambda_c^s + (6.3 C_1^{SM} + 5.4 C_2^{SM}) \lambda_u^s \end{aligned} \quad (31)$$

We discuss now the predictions of $C_7^{Z'}$ and $\tilde{C}_9^{Z'}$ in the LRS. We consider a case for which $Im(\Delta_R^{sb}) = Im(\Delta_L^{sb}) = 0$. In this case $C_7^{Z'} \equiv Re(C_7^{Z'})$ and $\tilde{C}_9^{Z'} \equiv Re(\tilde{C}_9^{Z'})$. In Fig.(4) left we show the contours of $Re(C_7^{Z'})$ ($Re(\tilde{C}_9^{Z'})$) in green (blue) color normalized by the SM Wilson coefficient C_9^{SM} . The shaded red regions are allowed from the bounds on ΔM_{B_s} for $M_{Z'} = 1$ TeV as discussed before. The contours of $Re(C_7^{Z'})$ ($Re(\tilde{C}_9^{Z'})$) are straight lines as $C_7^{Z'}$ ($\tilde{C}_9^{Z'}$) is a function of $Re(\Delta_L^{sb})$ ($Re(\Delta_R^{sb})$) only. Clearly from the figure $Re(C_7^{Z'})$ can reach a maximum value around $0.4 C_9^{SM}$ while $Re(\tilde{C}_9^{Z'})$ can reach a maximum value around $0.6 C_9^{SM}$. However $(Re(C_7^{Z'}), Re(\tilde{C}_9^{Z'})) = (0.4, 0.6)$ are excluded by the bounds on ΔM_{B_s} that require $Re(\Delta_R^{sb})$ and $Re(\Delta_L^{sb})$, and hence $Re(C_7^{Z'})$ and $Re(\tilde{C}_9^{Z'})$, not to be large simultaneously.

We consider another case where $Re(\Delta_R^{sb}) = Re(\Delta_L^{sb}) = 0$. In this case $C_7^{Z'} \equiv Im(C_7^{Z'})$ and $\tilde{C}_9^{Z'} \equiv Im(\tilde{C}_9^{Z'})$. In Fig.(4) right we show the contours of $Im(C_7^{Z'})$ ($Im(\tilde{C}_9^{Z'})$) in orange (magenta) color normalized by the SM Wilson coefficient C_9^{SM} . The shaded blue regions are allowed from the bounds on ΔM_{B_s} for $M_{Z'} = 1$ TeV. Recall that the constraints from $S_{\psi\phi}$ are so loose as discussed before. The conclusion for this case is the same as the previous case with just doing the replacements $Re(C_7^{Z'}) \rightarrow Im(C_7^{Z'})$ and $Re(\tilde{C}_9^{Z'}) \rightarrow Im(\tilde{C}_9^{Z'})$.

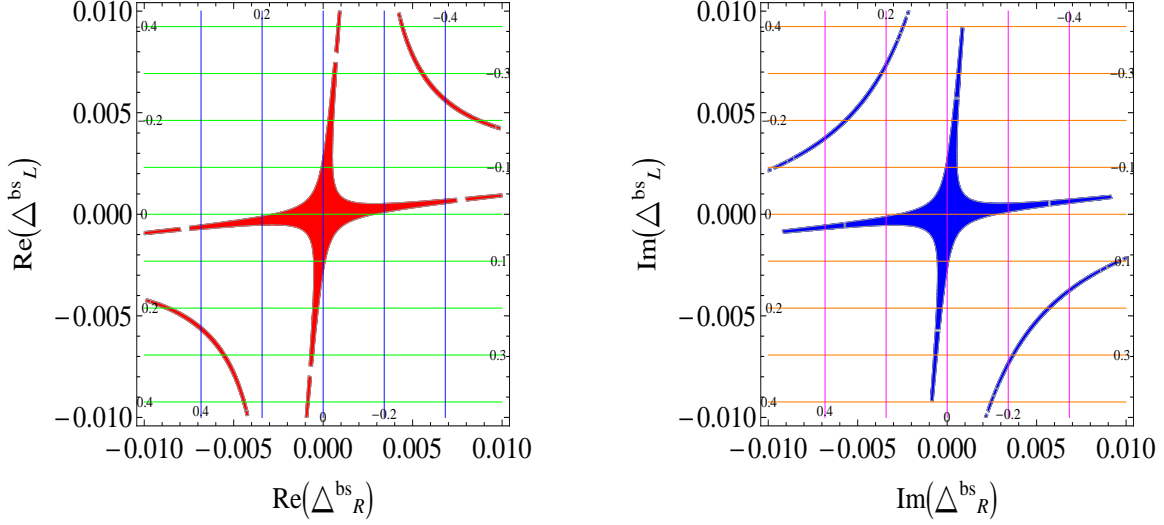


FIG. 4. Left: contours of $Re(C_7^{Z'})$ ($Re(\tilde{C}_9^{Z'})$) in green (blue) color normalized by the SM Wilson coefficient C_9^{SM} in the LRS corresponding to the case $Im(\Delta_R^{sb}) = Im(\Delta_L^{sb}) = 0$. Right: contours of $Im(C_7^{Z'})$ ($Im(\tilde{C}_9^{Z'})$) in orange (magenta) color normalized by the SM Wilson coefficient C_9^{SM} in the LRS corresponding to the case $Re(\Delta_R^{sb}) = Re(\Delta_L^{sb}) = 0$. In both plots the shaded colored regions are allowed from the bounds on ΔM_{B_s} for $M_{Z'} = 1$ TeV and .

We finally consider the general case where none of the real or imaginary parts of Δ_L^{sb} and Δ_R^{sb} is equal to zero. In Table IV we list the predictions of $C_7^{Z'}$ and $\tilde{C}_9^{Z'}$ corresponding to some sample sets of the parameter space allowed by both ΔM_{B_s} and $S_{\psi\phi}$ constraints for $M_{Z'} = 1$ TeV. As before, in obtaining these results we run each of the real and imaginary parts of Δ_L^{sb} and Δ_R^{sb} over the interval $[-0.01, 0.01]$ requiring that both ΔM_{B_s} and $S_{\psi\phi}$ constraints to be satisfied. From the Table we note that $Re(\tilde{C}_9^{Z'}) = Im(\tilde{C}_9^{Z'}) \simeq 0.6 C_9^{SM}$ corresponding to set III of the allowed parameter space. This is the maximum value of $Re(\tilde{C}_9^{Z'})(Im(\tilde{C}_9^{Z'}))$ obtained in our scan for all points in the parameter space that satisfy ΔM_{B_s} and $S_{\psi\phi}$ constraints. Regarding $C_7^{Z'}$ we find that $Re(C_7^{Z'})(Im(C_7^{Z'}))$ can reach a maximum value around $0.4 C_9^{SM}$.

Finally we turn to the predictions of the branching ratios of the processes under consideration. We start with $\bar{B}_s^0 \rightarrow \eta(\eta') \pi^0$ decays. Their related amplitudes are given in Eq.(30). Clearly the amplitude $\mathcal{A}_2(\bar{B}_s^0 \rightarrow \eta' \pi^0)$ has the largest coefficient of $\tilde{C}_9^{Z'}$ compared to the coefficients of both the $C_7^{Z'}$ and C_9^{SM} in the other amplitudes. As a result this amplitude receives the largest enhancement due to Z' contributions. In Fig.(5) left, we show the con-

Set	$Re(\Delta_L^{bs})$	$Im(\Delta_L^{bs})$	$Re(\Delta_R^{bs})$	$Im(\Delta_R^{bs})$	$Re(C_7^{Z'})$	$Im(C_7^{Z'})$	$Re(\tilde{C}_9^{Z'})$	$Im(\tilde{C}_9^{Z'})$
I	-0.01	-0.01	-0.001	-0.001	0.432943	0.432943	0.0586095	0.0586095
II	-0.01	0.005	-0.001	0.0005	0.432943	-0.216471	0.0586095	-0.0293047
III	-0.001	-0.001	-0.01	-0.01	0.0432943	0.0432943	0.586095	0.586095
IV	0.0035	-0.001	0.0095	0.005	-0.15153	0.0432943	-0.55679	-0.293047
V	0.0005	-0.001	0.005	-0.01	-0.0216471	0.0432943	-0.293047	0.586095

TABLE IV. Predictions of $C_7^{Z'}$ and $\tilde{C}_9^{Z'}$ corresponding to some sample sets of the parameter space for $M_{Z'} = 1$ TeV allowed by both ΔM_{B_s} and $S_{\psi\phi}$ constraints.

tours of $\mathcal{R}_2^{\pi^0\eta'}$ in the LRS for the case $Im(\Delta_L^{sb}) = Im(\Delta_R^{sb}) = 0$ where the shaded red regions satisfy the bounds on ΔM_{B_s} . In the same figure right, we show the contours of $\mathcal{R}_2^{\pi^0\eta'}$ for the case $Re(\Delta_L^{sb}) = Re(\Delta_R^{sb}) = 0$ where the shaded blue regions are allowed by the bounds on ΔM_{B_s} . In both plots we take $M_{Z'} = 1$ TeV. We see from the figure that $\mathcal{R}_2^{\pi^0\eta'}$ can reach a maximum value of about 2.5 in both cases.

In Table V we list the predictions of $\mathcal{R}_2^{\pi^0\eta'}$ corresponding to the general case where non of the real or imaginary parts of Δ_L^{bs} and Δ_R^{bs} is equal to zero and are allowed by both ΔM_{B_s} and $S_{\psi\phi}$ constraints. As before, in obtaining these results we run each of the real and imaginary parts of Δ_L^{sb} and Δ_R^{sb} over the interval $[-0.01, 0.01]$ requiring that both ΔM_{B_s} and $S_{\psi\phi}$ constraints to be satisfied for $M_{Z'} = 1$ TeV. From the Table we note that $\mathcal{R}_2^{\pi^0\eta'} \simeq 4.6$ corresponding to set I of the allowed parameter space. This means that Z' contributions can enhance the total branching ratio of $B_s^0 \rightarrow \pi^0 \eta'$ 4.6 times the SM prediction. This is the maximum value we obtained in our scan for all sets of the parameter space that satisfy both ΔM_{B_s} and $S_{\psi\phi}$ constraints.

We turn now to the decay modes $\bar{B}_s^0 \rightarrow \eta(\eta') \rho^0$. Their related amplitudes are given in Eq.(31). We note that the amplitude $\mathcal{A}_2(\bar{B}_s^0 \rightarrow \eta \rho^0)$ has the largest coefficient of $C_7^{Z'}$ compared to the coefficients of both the $\tilde{C}_9^{Z'}$ and C_9^{SM} in the other amplitudes. As a result this amplitude receives the largest enhancement due to Z' contributions. In Fig.(6) left, we show the contours of $\mathcal{R}_2^{\rho^0\eta}$ in the LRS for the case $Im(\Delta_L^{sb}) = Im(\Delta_R^{sb}) = 0$. In the same figure right, we show the contours of $\mathcal{R}_2^{\rho^0\eta}$ in the LRS for the case $Re(\Delta_L^{sb}) = Re(\Delta_R^{sb}) = 0$. In the figure the shaded colored regions satisfy the bounds on ΔM_{B_s} for $M_{Z'} = 1$ TeV. We see

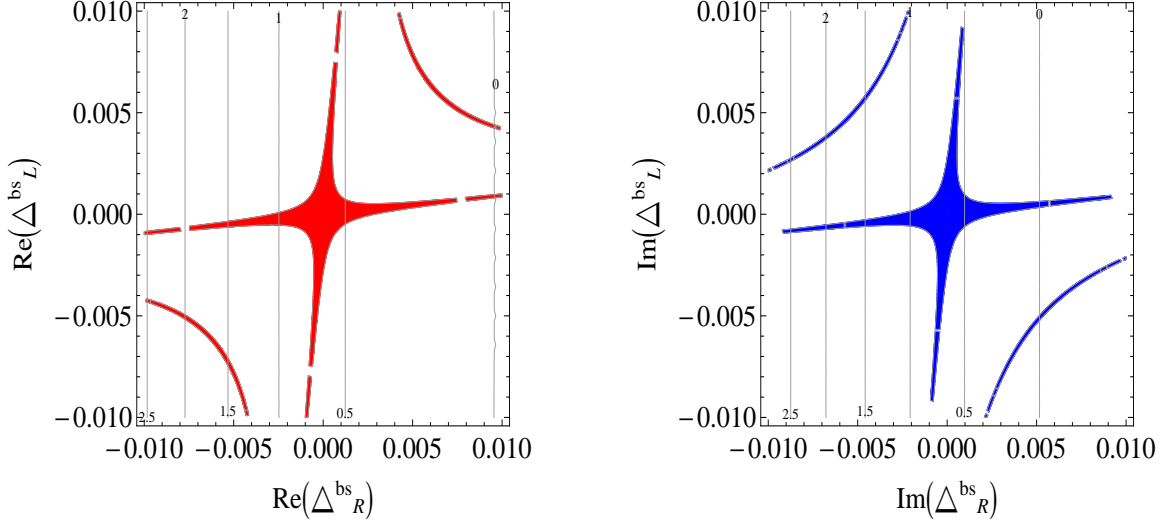


FIG. 5. Left: contours of $\mathcal{R}_2^{\pi^0 \eta'}$ in the LRS for the case $Im(\Delta_L^{sb}) = Im(\Delta_R^{sb}) = 0$. Right: contours of $\mathcal{R}_2^{\pi^0 \eta'}$ in the LRS for the case $Re(\Delta_L^{sb}) = Re(\Delta_R^{sb}) = 0$. In both plots the shaded colored regions satisfy the bounds on ΔM_{B_s} for $M_{Z'} = 1$ TeV.

from the figure that Z' contributions can enhance the total branching ratio of $B_s^0 \rightarrow \rho^0 \eta$ by about one order of magnitude comparing to the SM prediction. In fact this is the conclusion also for the general case where non of the real or imaginary parts of Δ_L^{bs} and Δ_R^{bs} is equal to zero as shown in Table VI. In that Table we list the predictions of $\mathcal{R}_2^{\rho^0 \eta}$ corresponding to some sample sets of the parameter space allowed by both ΔM_{B_s} and $S_{\psi\phi}$ constraints. As before, in obtaining these results we run each of the real and imaginary parts of Δ_L^{sb} and Δ_R^{sb} over the interval $[-0.01, 0.01]$ requiring that both ΔM_{B_s} and $S_{\psi\phi}$ constraints are satisfied at a value $M_{Z'} = 1$ TeV. From the Table we see that Z' contributions can enhance the total branching ratio of $B_s^0 \rightarrow \rho^0 \eta$ up to one order of magnitude comparing to the SM prediction.

Finally, from Fig.(6) we note that the enhancement of the branching ratios by an order of magnitude occurs in the regions in the parameter space corresponding to the thin branches in the figure. In these regions the $[\Delta S(B_s)]_{VLL(VRR)}$ and $[\Delta S(B_s)]_{LR}$ contributions to $B_s - \bar{B}_s$ mixing given in Eqs. (20,21) cancel each other to a large extent. For a proper interpretation of the given upper limit for the enhancement it is thus necessary to know the degree of fine-tuning between Δ_L^{sb} and Δ_R^{sb} for the corresponding points in the parameter space. For the case of real Δ_L^{sb} and Δ_R^{sb} , the fine-tuning can be quantified by the measure X_{B_s} introduced in eq.(26) in Ref.[58]. The corresponding expression reads

Set	$Re(\Delta_L^{bs})$	$Im(\Delta_L^{bs})$	$Re(\Delta_R^{bs})$	$Im(\Delta_L^{bs})$	$\mathcal{R}_2^{\pi^0 \eta'}$
I	-0.001	-0.001	-0.01	-0.01	4.6
II	-0.001	0.002	-0.0025	-0.01	3.3
III	0.0005	-0.001	0.002	-0.01	2.6
IV	-0.004	0.0005	-0.01	-0.0025	2.8
V	-0.001	0.0035	-0.001	-0.007	2.4

TABLE V. Predictions for $\mathcal{R}_2^{\pi^0 \eta'}$ corresponding to some sample sets of the parameter space for $M_{Z'} = 1$ TeV allowed by both ΔM_{B_s} and $S_{\psi\phi}$ constraints.

$$X_{B_s} = \frac{(\Delta_L^{sb})^2 + (\Delta_R^{sb})^2 - b_{B_s} \Delta_L^{sb} \Delta_R^{sb}}{(\Delta_L^{sb})^2 + (\Delta_R^{sb})^2 + b_{B_s} \Delta_L^{sb} \Delta_R^{sb}} \quad (32)$$

where

$$b_{B_s} = \frac{(\lambda_t^s)^2 g_{SM}^2}{4\tilde{r}T(B_s)} [C_1^{LR}(\mu_{Z'}) \langle Q_1^{LR}(\mu_{Z'}, B_s) \rangle + C_2^{LR}(\mu_{Z'}) \langle Q_2^{LR}(\mu_{Z'}, B_s) \rangle] \quad (33)$$

At $M_{Z'} = 1$ TeV we find that $b_{B_s} \simeq -10.8$. In Fig.(7) we show the points in the $\Delta_L^{sb} - \Delta_R^{sb}$ satisfying $X_{B_s} < 10$, $10 < X_{B_s} < 100$ and $100 < X_{B_s}$ in green, orange and blue colors respectively. All colored points satisfy the bounds on ΔM_{B_s} for $M_{Z'} = 1$ TeV. Clearly from Figs.(6,7) if we exclude points that lead to $100 < X_{B_s}$ from the parameter space and exclude their corresponding predictions of the branching ratios we still can have an enhancement by an order of magnitude. As before this enhancement occurs for rather fine-tuned points where ΔM_{B_s} constraint on $|S_{SM}(B_s) + S_{Z'}(B_s)|$ is fulfilled by overcompensating the SM via $S_{Z'}(B_s) \simeq -2S_{SM}(B_s)$. For instances this enhancement is still allowed for the the points lies on the thin red curved branch in Fig.(6) for which $\Delta_R^{sb} < -0.04$ and $\Delta_L^{sb} < -0.06$. In fact this conclusion agrees with the findings of Ref.[58] where they found that sizeable enhancements in the branching ratios of the process under their consideration are still possible for a fine-tuning of $X_{B_s} \leq 100$.

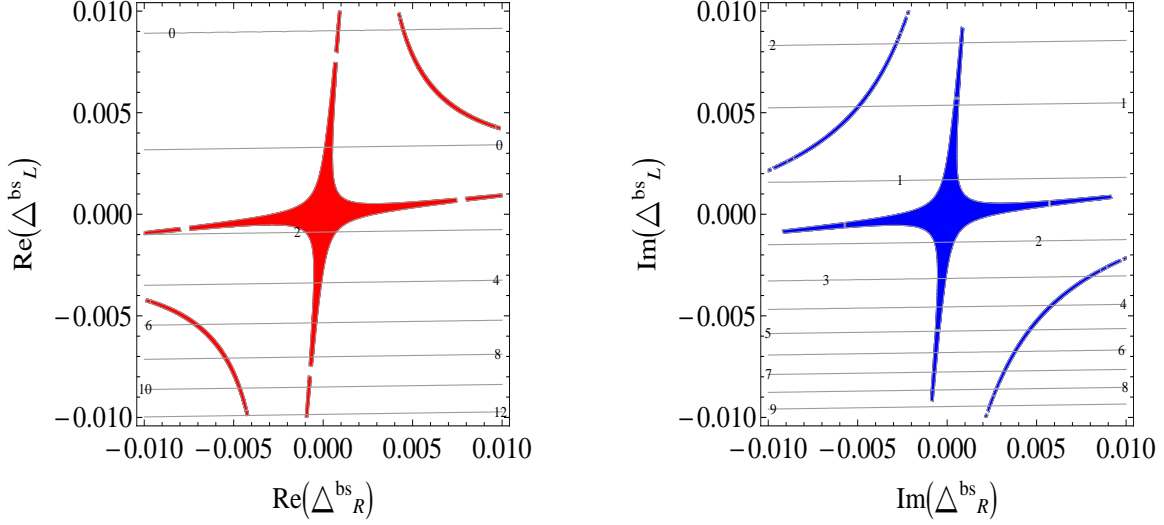


FIG. 6. Left: contours of $\mathcal{R}_2^{\eta\rho^0}$ in the LRS for the case $Im(\Delta_L^{sb}) = Im(\Delta_R^{sb}) = 0$. Right: contours of $\mathcal{R}_2^{\rho^0\eta}$ in the LRS for the case $Re(\Delta_L^{sb}) = Re(\Delta_R^{sb}) = 0$. In both plots the shaded colored regions satisfy the bounds on ΔM_{B_s} for $M_{Z'} = 1$ TeV.

V. CONCLUSION

In this work we have studied the decay modes $\bar{B}_s \rightarrow \pi^0(\rho^0)\eta^{(\prime)}$ within a model with an additional $U(1)'$ gauge symmetry and adopting SCET as a framework to calculate the amplitudes. We have derived the contributions to the amplitudes, within Soft Collinear Effective Theory, arising from new physics contributions to the weak effective Hamiltonian.

In the study we have considered a leptophobic Z' boson where its couplings to leptons vanish. Such a model can appear in models with an E_6 gauge symmetry. In this model Z' mass is much less constrained and the strongest constraints on the parameter space can be obtained by considering $B_s - \bar{B}_s$ mixing. We considered two scenarios, the Right-Handed Scenario, RHS, and Left-Right Scenario, LRS, based on the couplings of Z' to quarks that appear in the Wilson coefficients. In these scenarios we discussed the constraints on the parameter space from considering $B_s - \bar{B}_s$ mixing. As a consequence, we presented the predictions of the Wilson coefficients and accordingly the branching ratios of $\bar{B}_s \rightarrow \pi^0(\rho^0)\eta^{(\prime)}$.

In the RHS we found that the real part of $\tilde{C}_9^{Z'}$ can reach a maximum value of about 25% of C_9^{SM} . On the other hand the imaginary part of $\tilde{C}_9^{Z'}$ can reach a maximum value equal to C_9^{SM} . As a result we found that the decay amplitudes $\mathcal{A}_2(\bar{B}_s^0 \rightarrow \pi^0\eta')$ and $\mathcal{A}_2(\bar{B}_s \rightarrow$

Set	$Re(\Delta_L^{bs})$	$Im(\Delta_L^{bs})$	$Re(\Delta_R^{bs})$	$Im(\Delta_L^{bs})$	$\mathcal{R}_2^{\rho^0 \eta}$
I	-0.01	0.002	-0.001	0.0005	11.7
II	-0.01	-0.0025	-0.004	0.0005	13.3
III	-0.01	0.0035	-0.001	0.0005	11.6
IV	-0.0085	0.0035	-0.004	-0.001	9.3
V	0.002	-0.01	0.0005	-0.001	8.7
VI	-0.0025	-0.01	-0.001	0.002	11.5

TABLE VI. Predictions for $\mathcal{R}_2^{\rho^0 \eta}$ corresponding to some sample sets of the parameter space for $M_{Z'} = 1$ TeV allowed by both ΔM_{B_s} and $S_{\psi\phi}$ constraints.

$\rho^0 \eta'$) receive the largest enhancements due to the contributions of $\tilde{C}_9^{Z'}$ as they have the largest coefficients of the real and imaginary parts of $\tilde{C}_9^{Z'}$ compared to the other amplitudes. Accordingly we found that Z' contributions can enhance the total branching ratio of $\bar{B}_s^0 \rightarrow \pi^0 \eta'$ to six times the SM prediction while for $B_s^0 \rightarrow \rho^0 \eta'$ it is just 2.5 times the SM prediction. This kind of enhancement occurs for a rather fine-tuned point where ΔM_{B_s} constraint on $|S_{SM}(B_s) + S_{Z'}(B_s)|$ is fulfilled by overcompensating the SM via $S_{Z'}(B_s) \simeq -2S_{SM}(B_s)$. Moreover the constraint from $S_{\psi\phi}$ is also satisfied as Z' coupling to the b and s quarks is real at this point.

In the LRS the parameter space consists of the real and imaginary parts of Δ_L^{sb} and Δ_R^{sb} in addition to $M_{Z'}$. At a value of $M_{Z'} = 1$ TeV we scanned the real and imaginary parts of Δ_L^{sb} and Δ_R^{sb} over the interval $[-0.01, 0.01]$ requiring that both ΔM_{B_s} and $S_{\psi\phi}$ constraints to be satisfied. As a consequence we found that the maximum enhancements in the Z' Wilson coefficients correspond to $Re(\tilde{C}_9^{Z'}) = Im(\tilde{C}_9^{Z'}) \simeq 0.6 C_9^{SM}$ and $Re(C_7^{Z'}) = Im(C_7^{Z'}) \simeq 0.4 C_9^{SM}$. Regarding the branching ratios we found that Z' contributions can enhance the branching ratio of $B_s^0 \rightarrow \pi^0 \eta'$ by about 4.6 times the SM prediction. Moreover we found that the branching ratio of $B_s^0 \rightarrow \rho^0 \eta$ can be enhanced up to one order of magnitude comparing to the SM prediction for several sets of the parameter space satisfying both ΔM_{B_s} and $S_{\psi\phi}$ constraints and for a fine-tuning of $X_{B_s} \leq 100$. For these points ΔM_{B_s} constraint on $|S_{SM}(B_s) + S_{Z'}(B_s)|$ is fulfilled by overcompensating the SM via $S_{Z'}(B_s) \simeq -2S_{SM}(B_s)$.

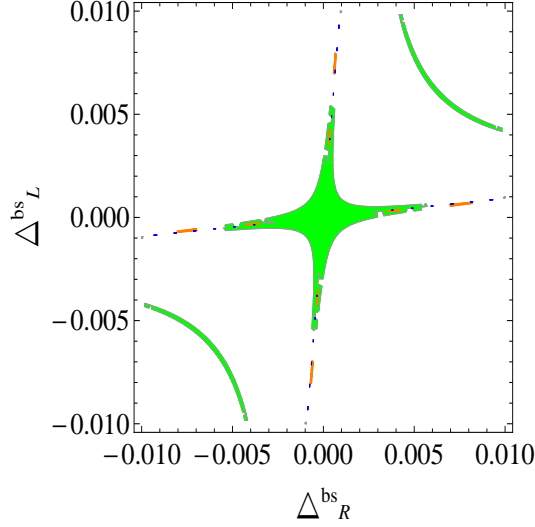


FIG. 7. Points satisfying $X_{B_s} < 10$, $10 < X_{B_s} < 100$ and $100 < X_{B_s}$ in green, orange and blue colors respectively. All colored points satisfy the bounds on ΔM_{B_s} for $M_{Z'} = 1$ TeV.

ACKNOWLEDGEMENTS

This work is supported by the research grant NTU-ERP-102R7701. I would like to thank prof. H. -Y. Cheng for useful discussions and his suggestion to do this study.

-
- [1] R. Fleischer, Phys. Lett. B **332**, 419 (1994).
 - [2] N. G. Deshpande, X. -G. He and J. Trampetic, Phys. Lett. B **345**, 547 (1995) [hep-ph/9410388].
 - [3] Y. -H. Chen, H. -Y. Cheng and B. Tseng, Phys. Rev. D **59**, 074003 (1999) [hep-ph/9809364].
 - [4] H. -Y. Cheng and C. -K. Chua, Phys. Rev. D **80**, 114026 (2009) [arXiv:0910.5237 [hep-ph]].
 - [5] M. Beneke and M. Neubert, Nucl. Phys. B **675**, 333 (2003) [hep-ph/0308039].
 - [6] L. Hofer, D. Scherer and L. Vernazza, JHEP **1102**, 080 (2011) [arXiv:1011.6319 [hep-ph]].
 - [7] A. Ali, G. Kramer, Y. Li, C. D. Lu, Y. L. Shen, W. Wang and Y. M. Wang, Phys. Rev. D **76**, 074018 (2007) [arXiv:hep-ph/0703162].
 - [8] W. Wang, Y. M. Wang, D. S. Yang and C. D. Lu, Phys. Rev. D **78**, 034011 (2008) [arXiv:0801.3123 [hep-ph]].

- [9] G. Faisel, JHEP **1208**, 031 (2012) [arXiv:1106.4651 [hep-ph]].
- [10] G. Faisel, Phys. Lett. B **731**, 279 (2014) [arXiv:1311.0740 [hep-ph]].
- [11] S. Descotes-Genon, J. Matias and J. Virto, Phys. Rev. D **88**, 074002 (2013) doi:10.1103/PhysRevD.88.074002 [arXiv:1307.5683 [hep-ph]].
- [12] R. Gauld, F. Goertz and U. Haisch, Phys. Rev. D **89**, 015005 (2014) doi:10.1103/PhysRevD.89.015005 [arXiv:1308.1959 [hep-ph]].
- [13] A. J. Buras and J. Girrbach, JHEP **1312**, 009 (2013) [arXiv:1309.2466 [hep-ph]].
- [14] R. Gauld, F. Goertz and U. Haisch, JHEP **1401**, 069 (2014) doi:10.1007/JHEP01(2014)069 [arXiv:1310.1082 [hep-ph]].
- [15] A. J. Buras, F. De Fazio and J. Girrbach, JHEP **1402**, 112 (2014) doi:10.1007/JHEP02(2014)112 [arXiv:1311.6729 [hep-ph]].
- [16] W. Altmannshofer, S. Gori, M. Pospelov and I. Yavin, Phys. Rev. D **89**, 095033 (2014) doi:10.1103/PhysRevD.89.095033 [arXiv:1403.1269 [hep-ph]].
- [17] Z. -j. Xiao, X. Liu and H. -s. Wang, Phys. Rev. D **75**, 034017 (2007) [hep-ph/0606177].
- [18] J. -f. Sun, G. -h. Zhu and D. -s. Du, Phys. Rev. D **68**, 054003 (2003) [hep-ph/0211154].
- [19] A. R. Williamson and J. Zupan, Phys. Rev. D **74**, 014003 (2006) [Erratum-ibid. D **74**, 03901 (2006)] [arXiv:hep-ph/0601214].
- [20] D. Zhang, Z. -j. Xiao and C. S. Li, Phys. Rev. D **64**, 014014 (2001) [hep-ph/0012063].
- [21] C. W. Bauer, S. Fleming and M. E. Luke, Phys. Rev. D **63**, 014006 (2000) [arXiv:hep-ph/0005275].
- [22] C. W. Bauer, S. Fleming, D. Pirjol and I. W. Stewart, Phys. Rev. D **63**, 114020 (2001) [arXiv:hep-ph/0011336].
- [23] J. Chay and C. Kim, Phys. Rev. D **68**, 071502 (2003) [arXiv:hep-ph/0301055].
- [24] J. Chay and C. Kim, Nucl. Phys. B **680**, 302 (2004) [arXiv:hep-ph/0301262].
- [25] C. W. Bauer, I. Z. Rothstein and I. W. Stewart, Phys. Rev. D **74**, 034010 (2006) [arXiv:hep-ph/0510241].
- [26] A. Jain, I. Z. Rothstein and I. W. Stewart, arXiv:0706.3399 [hep-ph].
- [27] C. Michael *et al.* [ETM Collaboration], Phys. Rev. Lett. **111**, no. 18, 181602 (2013) doi:10.1103/PhysRevLett.111.181602 [arXiv:1310.1207 [hep-lat]].
- [28] P. Ball and G. W. Jones, JHEP **0703**, 069 (2007) doi:10.1088/1126-6708/2007/03/069 [hep-ph/0702100 [HEP-PH]].

- [29] A. P. Bakulev, S. V. Mikhailov and N. G. Stefanis, Phys. Lett. B **578**, 91 (2004) doi:10.1016/j.physletb.2003.10.033 [hep-ph/0303039].
- [30] M. Masip and A. Pomarol, Phys. Rev. D **60**, 096005 (1999) [hep-ph/9902467].
- [31] E. Nardi, Phys. Rev. D **48** (1993) 1240 [hep-ph/9209223]; J. Bernabeu, E. Nardi and D. Tommasini, Nucl. Phys. B **409** (1993) 69 [hep-ph/9306251]; V. D. Barger, M. S. Berger and R. J. Phillips, Phys. Rev. D **52** (1995) 1663 [hep-ph/9503204]; M. B. Popovic and E. H. Simmons, Phys. Rev. D **62** (2000) 035002 [hep-ph/0001302]; T. G. Rizzo Phys. Rev. D **59** (1999) 015020 [hep-ph/9806397].
- [32] P. Langacker and M. Plumacher, Phys. Rev. D **62**, 013006 (2000) [hep-ph/0001204].
- [33] S. Chaudhuri, S. -W. Chung, G. Hockney and J. D. Lykken, Nucl. Phys. B **456**, 89 (1995) [hep-ph/9501361].
- [34] G. Cleaver, M. Cvetič, J. R. Espinosa, L. L. Everett and P. Langacker, Nucl. Phys. B **525**, 3 (1998) [hep-th/9711178].
- [35] G. Cleaver, M. Cvetič, J. R. Espinosa, L. L. Everett, P. Langacker and J. Wang, Phys. Rev. D **59**, 055005 (1999) [hep-ph/9807479].
- [36] Q. Chang, X. Q. Li and Y. D. Yang, J. Phys. G **41**, 105002 (2014) [arXiv:1312.1302 [hep-ph]].
- [37] W. Altmannshofer, A. J. Buras, D. M. Straub and M. Wick, JHEP **0904**, 022 (2009) [arXiv:0902.0160 [hep-ph]].
- [38] A. J. Buras, F. De Fazio and J. Girrbach, JHEP **1302**, 116 (2013) [arXiv:1211.1896 [hep-ph]].
- [39] A. J. Buras, F. De Fazio, J. Girrbach and M. V. Carlucci, JHEP **1302**, 023 (2013) [arXiv:1211.1237 [hep-ph]].
- [40] A. J. Buras, F. De Fazio, J. Girrbach, R. Knegjens and M. Nagai, JHEP **1306**, 111 (2013) [arXiv:1303.3723 [hep-ph]].
- [41] A. J. Buras, J. Girrbach and R. Ziegler, JHEP **1304**, 168 (2013) [arXiv:1301.5498 [hep-ph]].
- [42] A. J. Buras, R. Fleischer, J. Girrbach and R. Knegjens, JHEP **1307**, 77 (2013) [arXiv:1303.3820 [hep-ph]].
- [43] A. J. Buras, J. Girrbach-Noe, C. Niehoff and D. M. Straub, JHEP **1502**, 184 (2015) [arXiv:1409.4557 [hep-ph]].
- [44] P. Langacker, Rev. Mod. Phys. **81**, 1199 (2009) [arXiv:0801.1345 [hep-ph]].
- [45] Y. Grossman, M. Neubert and A. L. Kagan, JHEP **9910**, 029 (1999) [hep-ph/9909297].
- [46] P. Langacker and M. Plümacher, Phys. Rev. D **62** (2000) 013006 [hep-ph/0001204].

- [47] V. Barger, L. Everett, J. Jiang, P. Langacker, T. Liu and C. Wagner, Phys. Rev. D **80**, 055008 (2009) [arXiv:0902.4507 [hep-ph]].
- [48] Q. Chang, X. Q. Li and Y. D. Yang, JHEP **0905**, 056 (2009) [arXiv:0903.0275 [hep-ph]].
- [49] V. Barger, L. L. Everett, J. Jiang, P. Langacker, T. Liu and C. E. M. Wagner, JHEP **0912**, 048 (2009) [arXiv:0906.3745 [hep-ph]].
- [50] V. Barger, L. Everett, J. Jiang, P. Langacker, T. Liu and C. Wagner, JHEP **0912** (2009) 048 [arXiv:0906.3745].
- [51] C. W. Chiang, Y. F. Lin, Jusak Tandean, JHEP **1111** (2011) 083 [arXiv:1108.3969].
- [52] T. G. Rizzo, Phys. Rev. D **59**, 015020 (1998) [hep-ph/9806397].
- [53] A. J. Buras, S. Jager and J. Urban, Nucl. Phys. B **605**, 600 (2001) [hep-ph/0102316].
- [54] A. J. Buras and J. Girrbach, JHEP **1203**, 052 (2012) [arXiv:1201.1302 [hep-ph]].
- [55] Y. Amhis *et al.* [Heavy Flavor Averaging Group Collaboration], arXiv:1207.1158 [hep-ex].
- [56] S. Chatrchyan *et al.* [CMS Collaboration], Phys. Lett. B **720**, 63 (2013) [arXiv:1212.6175 [hep-ex]].
- [57] P. Clarke, Results on CP-violation in Bs Mixing, LHCb-TALK-2012-029, CERN, Geneva Switzerland (2012).
- [58] A. Crivellin, L. Hofer, J. Matias, U. Nierste, S. Pokorski and J. Rosiek, Phys. Rev. D **92**, no. 5, 054013 (2015) doi:10.1103/PhysRevD.92.054013 [arXiv:1504.07928 [hep-ph]].